ROTORDYNAMIC STABILITY TESTS ON HIGH-PRESSURE RADIAL COMPRESSORS

by

Urs Baumann

Manager, Mechanical Development

Sulzer Turbo Ltd.

Zurich, Switzerland

Urs Baumann is the Manager of the Mechanical Development department of Sulzer Turbo Ltd., in Zurich, Switzerland. His responsibilities include the mechanical improvement of turbocompressors and associated components, as well as the implementation and maintenance of test stands and analytical tools needed to fulfill this task.

Before joining Sulzer Turbo in 1996, Mr. Baumann worked for Sulzer Innotec, the Corporate Research and Development Center. For several years, he was in charge of the machinery dynamics group that is responsible for the development, design improvement, and troubleshooting on a wide range of Sulzer products.

Mr. Baumann has a diploma (Mechanical Engineering, 1987) from the Swiss Federal Institute of Technology in Zurich.

ABSTRACT

This paper describes extensive measurements on high-pressure radial compressors with rated discharge pressures of more than 400 bar (5800 psi). The purpose of the measurements was to determine the damping behavior of the entire machines as a function of several parameters such as discharge pressure, bearing distance, labyrinth types, or configurations of anti-swirl devices.

In the past, most of the rotordynamic damping measurements have been carried out by universities on test rigs specially designed to measure labyrinth forces, which are mainly responsible for the change in damping at high pressures. Unfortunately, all these tests have been carried out at pressure levels far below the levels of industrial applications. Thus, the presented tests on complete compressors, ready for offshore applications, are certainly unique. The tests showed a generally conservative prediction of the damping. At higher pressures, a drop of the first natural frequency of the shaft was encountered. This effect could be attributed to the used labyrinth type.

INTRODUCTION

In recent years, analytical tools have been developed to predict the damping of labyrinth seals (Wyssmann, et al., 1984; Nordmann and Weiser, 1988; Weiser, 1989). Numerous experimental investigations were carried out to determine the impact of different labyrinth seal configurations on the rotordynamic behavior of the rotor (Childs and Scharrer, 1986a; Childs, et al., 1986b; FVV Report, 1990). With these results, the codes were adjusted for an optimal prediction of the used labyrinth seals. In the present design of Sulzer high-pressure compressors, anti-swirl devices are installed at all stages in order to achieve sufficient rotordynamic stability. In this case, the analyses indicate very high damping for the entire machine. According to these results, sufficient damping can be maintained with the elimination of at least some of the anti-swirl devices. In the case of high-pressure/small volume flow compressors, this would have a dramatically positive impact on the thermodynamic efficiency.

The primary goal of the measurements was to check the analytical predictions and to determine more accurate design rules for the installation of the necessary anti-swirl devices.

HIGH-PRESSURE COMPRESSOR DESIGN

The author's company's high-pressure compressors are designed as inline machines with five to seven stages and a balance piston to control the resulting thrust. Figure 1 shows a typical barrel type compressor. In the range of discharge pressures around 400 bar (5800 psi), the shaft is sealed against the environment by a triple dry gas seal cartridge. The lightweight rotor is supported by tilting pad journal bearings ensuring a good rotordynamic stability at unloaded conditions. The normal train design features a solid quillshaft coupling between gearbox and compressor, as well as a thrust bearing within the gearbox at the low speed shaft end. Figure 2 gives a schematic of a typical train arrangement showing the single helical toothing of the gearbox. The axial forces are transmitted from the compressor to the low speed shaft by means of thrust collars on the pinion.

One of the main issues in the design of high-pressure compressors is the balance between rotordynamic stability and thermodynamic performance. This balance is mainly influenced by the high density gas leaking through different types of internal sealing labyrinths. In high-pressure applications, the stabilizing or destabilizing labyrinth forces can be significantly higher than the stabilizing bearing forces that are always present (independent of the pressure). Therefore, special attention must be paid to the design of the sealing labyrinths to have no adverse influence on the overall stability of the compressor.

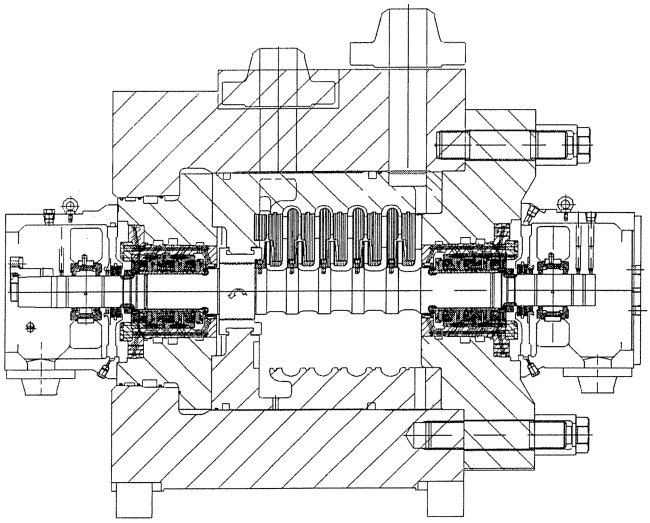

Figure 1. Cross Section of a High Pressure Gas Injection Compressor.

Labyrinth Types

Since the internal leakage influences the efficiency of the compressor, it has to be minimized by an appropriate design.

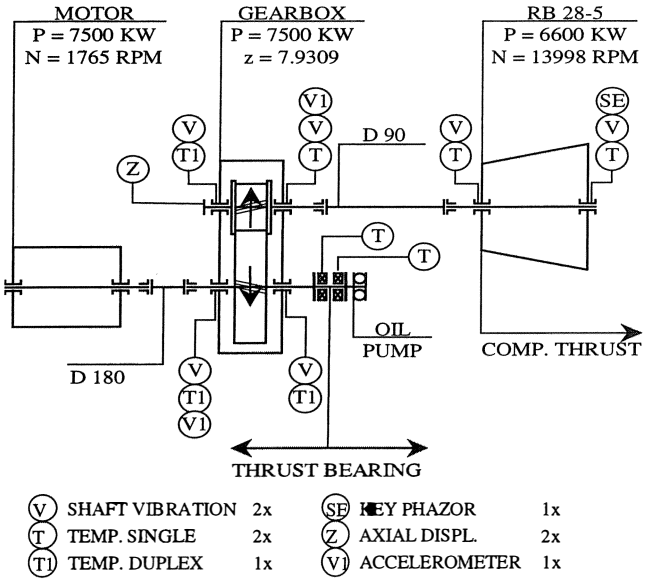

Figure 2. Schematic of a Compressor Train Arrangement.

Figure 3 shows the different labyrinth types used in high-pressure applications. Comb-grooved labyrinths have a significantly lower leakage flow than smooth labyrinths. The biggest disadvantage of this type of seal is a certain risk of having thrust temperature dependent labyrinth coefficients (axial position). The main application of the comb-grooved labyrinth is the balance piston, sealing the highest differential pressure and therefore having the biggest impact on the efficiency. On the hub and the shroud seals, either smooth or comb-grooved labyrinths can be used.

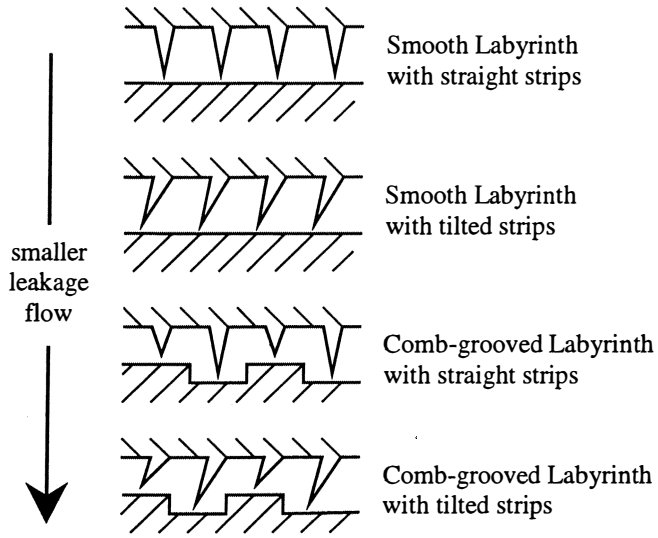

Figure 3. Labyrinth Seals Used in High Pressure Applications.

Tilted labyrinth strips always reduce the leakage flow in comparison to straight strips. Unfortunately there are no experimental data available to show that the tilted surfaces do not adversely influence the seal coefficients. All the available analytical tools (Wyssmann, et al., 1984, "bulk flow;" Weiser, 1989, "finite differences") assume rectangular grids and therefore neglect the tilting of the strips.

Influence of Swirl on Stability

The potentially destabilizing tangential forces are determined mainly by the relative circumferential speed of the gas within the labyrinth. This tangential seal force can be written as:

$$F_\theta = r_0 \cdot (K_{XY} - C_{XX} \cdot \omega) \tag{1}$$

where r_0 is the radius of the circular, synchronous orbit and ω is the precessional speed of the shaft. C_{XX} and K_{XY} are the direct damping and the cross-coupling stiffness coefficients, respectively. Equation (1) can be rewritten as follows:

$$F_\theta = -C_{XX} \cdot r_0 \cdot \omega \cdot \left(1 - \frac{K_{XY}}{C_{XX} \cdot \omega}\right) = -C_{eff} \cdot r_0 \cdot \omega \tag{2}$$

where C_{eff} is the equivalent effective damping coefficient of the labyrinth seal. This leads to the following definition of C_{eff}:

$$C_{eff} = C_{XX} \cdot \left(1 - \frac{K_{XY}}{C_{XX} \cdot \omega}\right) \tag{3}$$

At the threshold of stability, the precessional speed of the shaft becomes equal to the lowest critical speed. This leads to the following definition of the swirl frequency ratio based on the critical speed (SFR_ω):

$$SFR_\omega = \frac{K_{XY}}{C_{XX} \cdot \omega} \tag{4}$$

Extending Equation (4) with the rotational speed (Ω) of the shaft leads to:

$$SFR_\omega = \frac{K_{XY}}{C_{XX} \cdot \Omega} \cdot \frac{\Omega}{\omega} = SFR_\Omega \cdot FR \tag{5}$$

where SFR_Ω is the swirl frequency ratio based on the rotational speed of the shaft and FR is the flexi ratio, which is a measure of the flexibility of the shaft at the speed of operation. Figure 4 visualizes the stability criterion given in Equation (3). A labyrinth seal is stabilizing if the shaft is driving the gas, and it is destabilizing if the gas is pushing (exciting) the shaft.

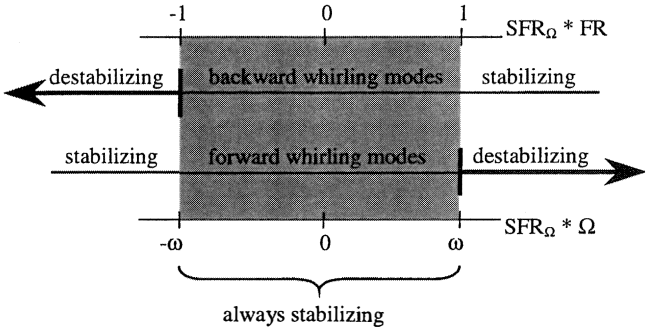

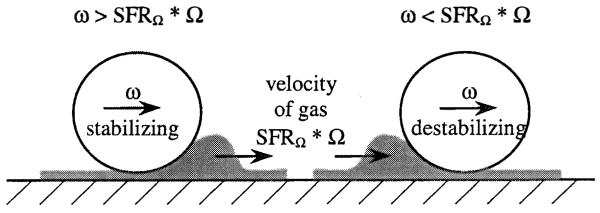

Figure 4. Stability Criterion of Labyrinth Seals.

Swirl Brakes

The swirl frequency ratio based on the rotational speed of the shaft can also be defined as the ratio of the average swirl of the

labyrinth flow to the rotational speed of the shaft (relative average swirl):

$$SFR_{\Omega} = \frac{K_{XY}}{C_{XX}} \cdot \frac{1}{\Omega} = \frac{swirl}{\Omega} \qquad (6)$$

The installation of swirl brakes significantly reduces the swirl within the labyrinth. In some cases the swirl even becomes negative, causing the labyrinth to be a very strong source of damping (C_{eff}). The author's company uses two different types of swirl brakes. The first is a conventional type consisting of a certain number of radial slots placed directly in front of the labyrinth seal entrance. This type ensures a zero preswirl to the seal. The second type is called a thrust brake, again consisting of a certain number of radial slots, but placed on the outer diameter of the shroud sideroom. The thrust brake reduces the swirl in the sideroom and therefore also at the entrance to the labyrinth. This results in a higher pressure in the shroud sideroom, which compensates the impeller thrust and reduces the overall thrust of the compressor. On the other hand, the higher pressure in the sideroom leads to an increased leakage flow and therefore to a lower performance of the compressor. Figure 5 shows the different types of swirl brakes used in high-pressure compressors.

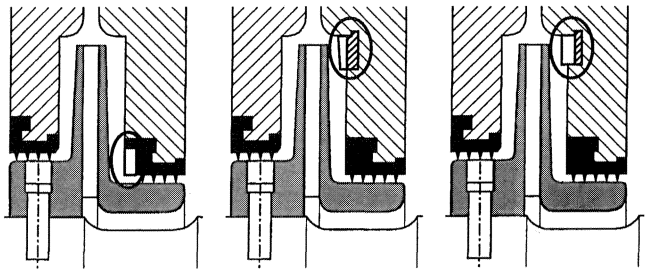

Figure 5. Swirl and Thrust Brakes Used in High Pressure Compressors.

Extensive inhouse measurements and finite difference (FD) calculations were undertaken to determine the preswirl for all relevant configurations. Tables 1 and 2 give a rough overview of the preswirl to be expected for the most relevant geometries and the average relative swirls within the labyrinths.

Table 1. Inlet Swirls as a Function of the Type of Swirl Brakes Installed.

Location of Labyrinth	Type of Swirl Brake	Labyrinth Strips at Stator	Labyrinth Strips at Rotor
Shroud Disk	No Swirl Brake	75 %	75 %
	Swirl Brake	0 %	0 %
	Thrust Brake Type 1	15 %	15 %
	Thrust Brake Type 2	35 %	35 %
Hub Disk	No Swirl Brake	10 %	15 %

TEST SETUP

To verify the analytically predicted damping within high-pressure compressors, a first machine was modified and measured in December 1996 (ULA 96). The results of these measurements led to a second identical measuring campaign with a similar machine in May 1998 (ALWYN 97).

Main Compressor Data

Since both testing campaigns were carried out on customer owned injection machines, all modifications had to be executed with utmost care to ensure the complete integrity of the compressors during the tests and also later in their offshore applications. Table 3 gives the main compressor data for the two modified and tested machines.

Table 2. Average Relative Swirls as a Function of the Inlet Swirl and the Type of the Labyrinth.

Type of Labyrinth	Type of Swirl Brake	Location of Labyrinth: Shroud Disk ~4-5 Strips	Location of Labyrinth: Balance Pist. ~11 Strips
Smooth with Stator Strips	No Swirl Brake	+90 %	+60 %
	Swirl Brake	-45 %	-45 %
	Thrust Brake Type 1	-20 %	-
	Thrust Brake Type 2	+5 %	-
Comb-Grooved with Stator Strips	No Swirl Brake	+75 %	~+100 %
	Swirl Brake	-15 %	~0%
	Thrust Brake Type 1	0 %	-
	Thrust Brake Type 2	+25 %	-

Since the analytical predictions indicated very high damping for most of the possible configurations to be tested, a shaft extension was designed that allowed the tests to be carried out with both the normal and an extended bearing span. Figure 6 shows the modified nondrive end (NDE) of the shaft with the two alternative bearing locations.

Table 3. Main Compressor Data of the Two Tested Machines.

Feature	Units	ULA	ALWYN
Number of Stages	-	6	5
Rotor Mass	kg (lb)	180 (397)	168 (370)
Normal Bearing Span	mm (in)	1290 (50.8)	1305 (51.4)
Extended Bearing Span	mm (in)	1550 (61.0)	1620 (63.8)
Bearing Diameter	mm (in)	80 (3.15)	90 (3.54)
Shaft Dia at Impellers	mm (in)	130 (5.12)	130 (5.12)
Nat.Freq. at full Speed (norm)	Hz	100	100
Nat.Freq. at full Speed (ext.)	Hz	70	70
Rated Speed	rpm	14141	13998
Maximum Discharge Pressure	bar (psi)	450 (6525)	440 (6380)
Disch. Temp. near Oprimum	°C (°F)	160 (320)	152 (306)
Pressure Ratio near Optimum	-	2.5	2.4
Test Gas	g/mol	N2 - 28	N2 - 28

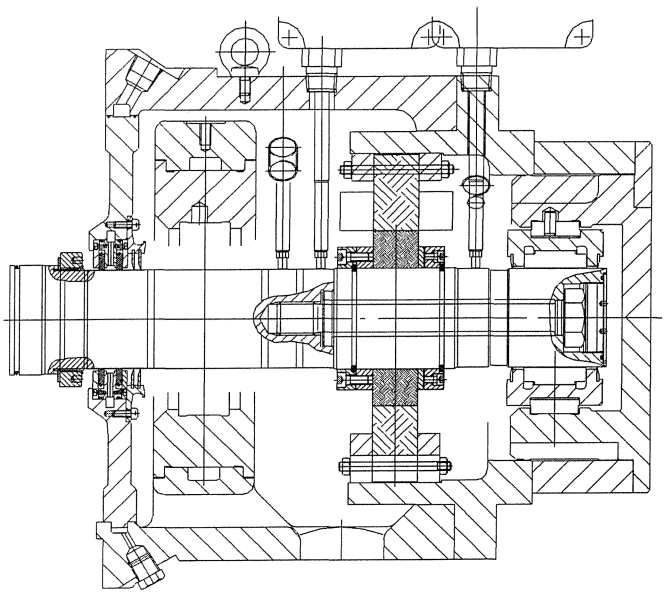

Figure 6. Compressor Shaft NDE with Additional Extension Showing the Two Alternative Bearing Positions, the Location of Excitation, and the Probe Locations.

Excitation

To determine the overall damping of the compressor at normal operation, it is necessary to provide an excitation to the rotor that is frequency-independent from the rotor speed. For this purpose, an electromagnetic exciter was installed between the two alternative bearing locations. This exciter produced forces only in a horizontal direction. Table 4 gives a listing of the main characteristic data of the exciter used. With this force arrangement, all modes of the rotor were excited, i.e., the forward and the backward whirling modes. For the stability of the shaft, the damping of the lowest bending mode is relevant. Therefore, the shaft vibration measurement must be able to show clear responses of this mode. The shapes of the first bending modes are shown in Figure 7 for both bearing locations. The best evaluations of the shaft responses were always obtained from the measuring plane *c*.

Table 4. Main Exciter Data.

Feature	Units	ULA and ALWYN
Radial Air Gap	mm (in)	0.550 (0.022)
Maximum Harmonic Current	A ptp	14
Maximum Harmonic Force	N ptp	3000
Current to Control Voltage	A ptp / V eff	5
Force to Control Voltage	N ptp / V eff	~1000

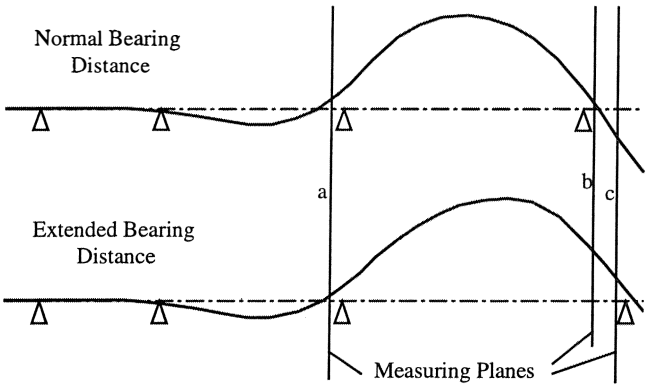

Figure 7. Modeshapes of the Lowest Bending Modes for Normal and Extended Bearing Span.

Tested Configurations

The first machine (ULA 96) was equipped with comb-grooved labyrinths with tilted stator strips throughout the whole compressor. In the second machine (ALWYN 97), the comb-grooved labyrinth was used only within the balance piston, the impeller labyrinths were all smooth. Throughout the whole machine, straight stator strips were used (except for one tested configuration, ALW.5, where the balance piston labyrinth was replaced with a type with tilted strips). Table 5 gives a list of all tested configurations.

Procedure of Tests

All tests were carried out at the rated speed of the appropriate compressor. In all configurations, the pressure was raised either to the maximum reachable discharge pressures of around 400 bar to 450 bar (5800 psi to 6500 psi) or to the maximum discharge pressure at the threshold of stability. All tests were carried out with pure nitrogen and the pressure ratio of the compressor was varied between 1.6 (near choke) and 2.5 (near surge).

The excitation was a harmonic force performing a stepped sweep from approximately 40 Hz to 150 Hz. The level of excitation was adjusted for each configuration, in order to achieve useful responses during resonance with the first critical speed. For an operating point near the optimum, the damping values were calculated for all measured configurations. Figure 8 shows the expected damping for all tested configurations. It can clearly be seen that, according to the predictions, it would be sufficient to have the swirl brakes installed only at the balance piston and one or two stages. The ALWYN compressor shows analytically a slightly higher damping than ULA.

Table 5. Tested Configurations.

Config.	Bearing Span	Thrust Brakes at Stage						Swirl Brake at Balance Piston	Remarks
		1	2	3	4	5	6		
ULA.1	norm.	x	x	x	x	-	-	x	
ULA.2	norm.	x	x	-	-	-	-	x	
ULA.3	norm.	-	-	-	-	-	-	x	
ULA.4	ext.	-	-	-	-	-	-	x	
ULA.5	ext.	-	-	x	-	x	x	x	
ALW.1	norm.	x	x	-	-	-	*	-	
ALW.2	ext.	x	x	-	-	-	*	-	
ALW.3	ext.	x	x	-	-	-	*	x	
ALW.4	norm.	x	x	x	x	-	*	x	**
ALW.5	norm.	x	x	x	x	-	*	x	**
ALW.6	norm.	x	x	x	x	x	*	x	

* ALWYN has only 5 stages

** ALW.4 with straight, ALW.5 with tilted strips at balance piston

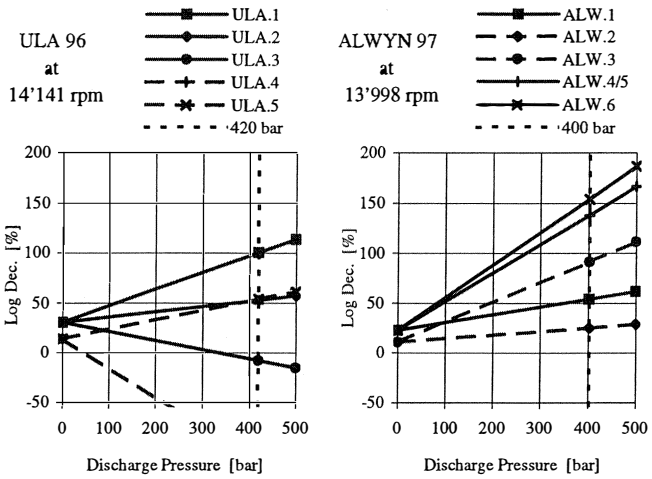

Figure 8. Expected Damping for All Tested Configurations as a Function of the Discharge Pressure.

TEST RESULTS

The most surprising result of the whole test series is a remarkable drop of the first bending mode in some of the tested configurations. Figure 9 shows one example for this observation. The drop of the first bending mode could be observed in all configurations that included swirl brakes at all or almost all stages. Whereas in configurations with no or only a few swirl brakes, no such effect was encountered.

In all cases without frequency drop, the damping and the threshold of stability were determined quite accurately, always showing a somewhat underestimated damping and threshold pressure. Figure 10 shows the measured damping and stability threshold for configuration ULA.3. Table 6 gives a list of all configurations where an unstable behavior was encountered. The good prediction in these cases allows the conclusion that all considered labyrinth forces in circumferential direction, i.e., cross coupling stiffness and direct damping, are calculated more or less correctly.

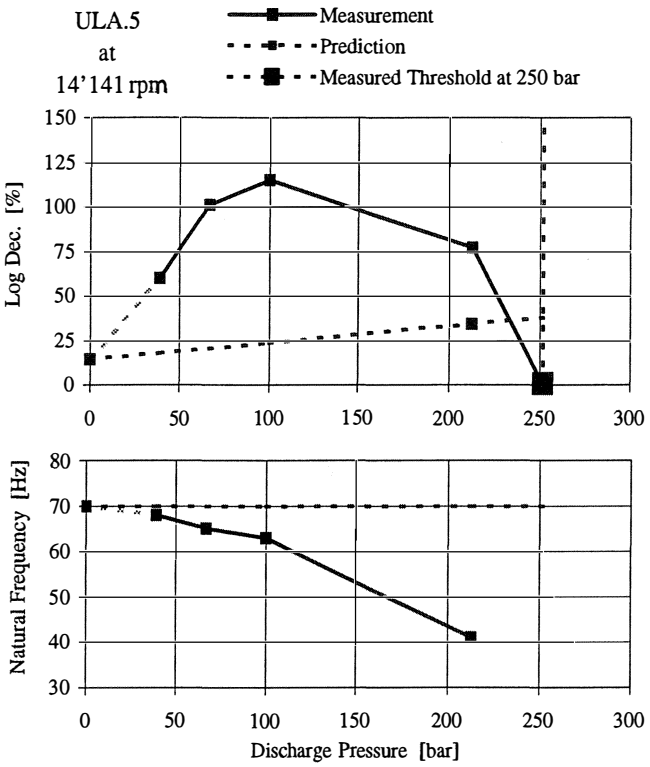

Figure 9. Measured Natural Frequency and Damping for Configuration ULA.5 Showing a Considerable Drop of the First Bending Mode of the Shaft.

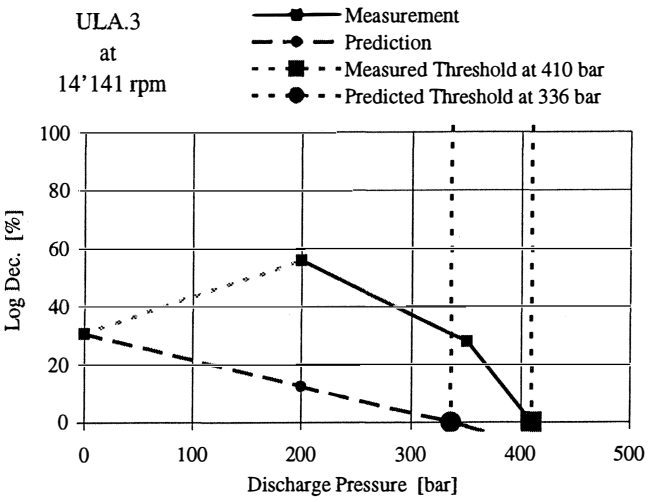

Figure 10. Measured and Predicted Damping and Threshold of Stability (ULA.3) Indicating Conservative Analytical Results.

Table 6. Measured and Calculated Threshold of Stability at Rated Speed.

Config	Threshold at p_out bar (psi)		Remarks
	Measured	Predicted	
ULA.3	420 (6090)	350 (5080)	
ULA.4	95 (1380)	45 (650)	
ULA.5	250 (3630)	none	freq. drop to ~40 Hz
ALW.2	none	none	near opt. point
	71 (1030)	105 (1520)	near choke

However, in those cases with a measured frequency drop, the calculated radial labyrinth seal forces seem to deviate from reality. Or more precisely, the calculations do not show this special effect that causes the first bending mode to drop. Therefore the analytical model is not able to predict the observed behavior of the natural frequency and damping. In Figure 9, it can be seen that the damping rises for lower pressures as predicted and drops again above a certain pressure. The natural frequency drops more or less steadily over the whole pressure range.

In the past, attention was paid mainly to the labyrinth forces in circumferential direction, since they directly influence the damping (Equation (3)). However, the measured results indicate that the forces in radial direction are important as well because their influence on the first bending mode (ω) can be very big, thus having an important secondary impact on the stability of the rotor.

Miscellaneous Findings

Hysteresis Effect

When crossing the threshold of stability, the damping shows a distinct hysteretic behavior. This can clearly be seen in Figure 11 for configuration ULA.4, where no swirl brakes are present at the impellers. Obviously it is possible to cross the threshold of stability with the rotor still having some damping. Suddenly the rotor becomes unstable and it is not possible to regain stability until the pressure drops below the threshold. It has to be noted that all damping values in this example are at a very low level.

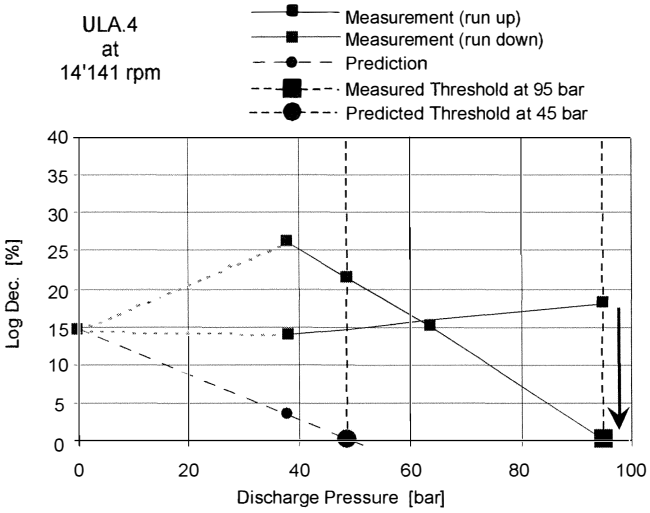

Figure 11. Measured and Predicted Damping for an Unstable Configuration (ULA.4) Showing a Distinct Hysteresis at the Threshold of Stability.

Operating Points Near Choke

At operating points very close to choke, the measured damping is considerably smaller than that calculated for the optimum point. At these operating conditions, the diffuser does not produce a pressure gain anymore, causing the flow in the hub disk labyrinth to change direction. The higher preswirl in this case causes the hub disk labyrinth to have a destabilizing influence. This effect could be verified with configuration ALW.2. Figure 12 shows the comparison of the measured and predicted damping for this case. Here also it has to be noted that all damping values in this example are at a very low level. This is the only case where the prediction (with backward flow in the hub labyrinth) does not give a conservative result.

Straight Versus Tilted Labyrinth Strips

The influence of the angle of the labyrinth strips has been investigated by a comparison between the configurations ALW.4

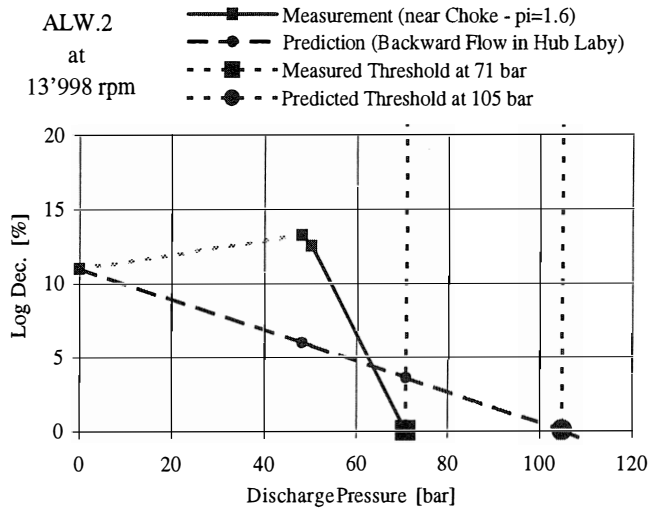

Figure 12. Measured and Predicted Damping for an Operating Point near Choke (ALW.2).

(straight strips throughout the machine) and ALW.5 (tilted strips at the balance piston). Both labyrinths show a moderate drop of the first bending mode, with the tilted strip labyrinth dropping somewhat less. As a consequence of this, the damping of the tilted strip labyrinth shows a slightly higher ascending gradient. Figure 13 shows the measured data together with the analytical prediction.

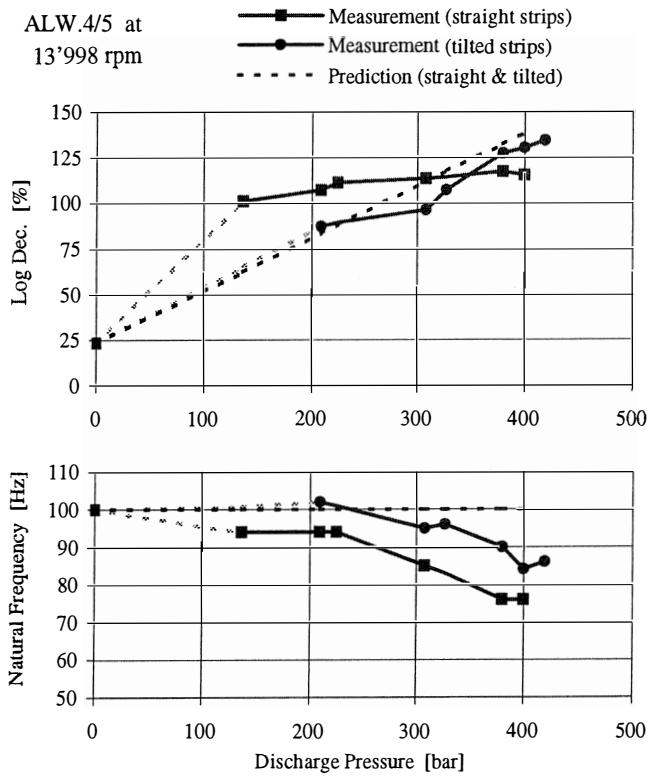

Figure 13. Comparison Between a Balance Piston with Straight and with Tilted Strips (ALW.4/ALW.5).

Smooth Versus Comb Grooved Labyrinths

This is more or less a comparison between the two measured machines, ULA with comb-grooved labyrinths in the impeller seals and ALWYN with smooth labyrinths. Figure 14 shows the comparison between ULA.1 and ALW.4. In both configurations, the first four stages are equipped with swirl brakes. Figure 14 indicates clearly that ULA.1 shows a much more distinct drop of the first bending mode than ALW.4. This allows the conclusion that smooth labyrinths are far less sensitive to the effects that cause the observed frequency drop. The comparison of all available measurements from the two machines leads to the conclusion that the observed frequency drop is most probably caused by the comb-grooved labyrinths. Since this effect correlates with the presence of swirl brakes, two possible causes can be identified. First, a small preswirl has an unexpected impact on the radial seal coefficients of a comb-grooved labyrinth. Or second, the different number of swirl brakes produce very different thrust conditions that result in different axial positions of the shaft. In a comb-grooved labyrinth, the axial position is obviously an important factor since the size and the shape of the labyrinth chambers are affected. It was planned to verify this second point by the measurement of the axial position of the shaft (ALWYN 97). Unfortunately, the setup in the test stand turned out to be more flexible in axial direction than expected. Therefore the axial measurement at the gearbox did not give very accurate axial positions of the shaft within the compressor casing. Nevertheless it was possible to qualitatively determine the axial positions of the shaft. The comparison of these measurements with the results of an FD calculation will be discussed later.

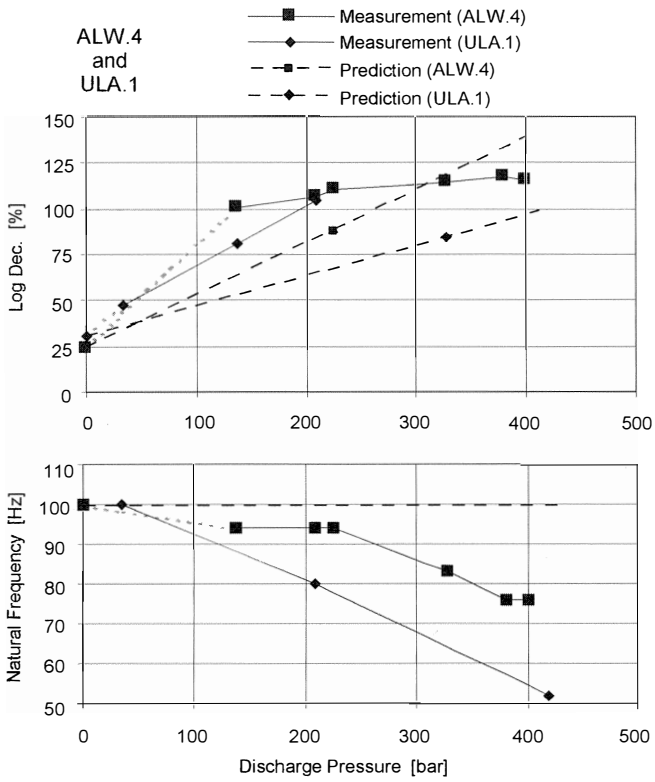

Figure 14. Comparison Between Smooth and Comb-Grooved Impeller Labyrinths (ALW.4/ULA.1).

A third possible reason for the observed frequency drop could be identified as the impeller-diaphragm interaction within the shroud sideroom. The flow pattern within the sideroom is completely different if a thrust brake is present or not. Presently there are some severe doubts if this interaction is able to produce sufficiently high radial coefficients. The further investigation of this possibility is not the subject of the present paper.

Influence of the Thrust on the Finally Chosen Configuration

In the case of ULA, the machine was delivered to the customer with thrust brakes only in the stages 3, 5, and 6, which is equivalent to the configuration ULA.5, but of course with normal bearing

span. With this arrangement, the efficiency of the compressor could be increased by approximately 6 percent to 8 percent, compared with the original layout. In the case of ALWYN, which of course was the machine with the higher measured damping and a much lower frequency drop, it was necessary to keep all the thrust brakes in the machine. The reason for this was the overall thrust of the machine, which had to be within the limits of the thrust bearing for all expected operating conditions. With a thrust layout of the machine with only a few thrust brakes (as much as necessary, if the prediction is accurate), it would have been possible to gain at least 8 percent of efficiency.

CALCULATIONS

FD Calculations

A series of FD calculations was carried out to investigate analytically the influence of the axial position of the rotor with respect to the stator of the labyrinth. Figure 15 shows the flow patterns for two different axial positions of the shaft. When the strip is centered within the groove (and on the comb) two vortices show up. When the strip is moved against the flow toward the edge of the comb, a sudden change of the flow pattern occurs and only the big vortex within the groove survives. The comparison of the radial seal coefficients in these cases reveals that the axially displaced position has strongly positive direct stiffness, whereas the centered position shows negative direct stiffness coefficients. All other coefficients seem to be more or less indifferent to the axial positions. The order of magnitude of the negative stiffness coefficients was far too small (approximately a factor of 10) to explain the measured frequency drop. However, the comparison of these results with the measured natural frequencies and the corresponding estimated axial positions showed a very poor correlation. Therefore the axial position of the shaft within the labyrinth could not be verified as the root cause of the frequency drop.

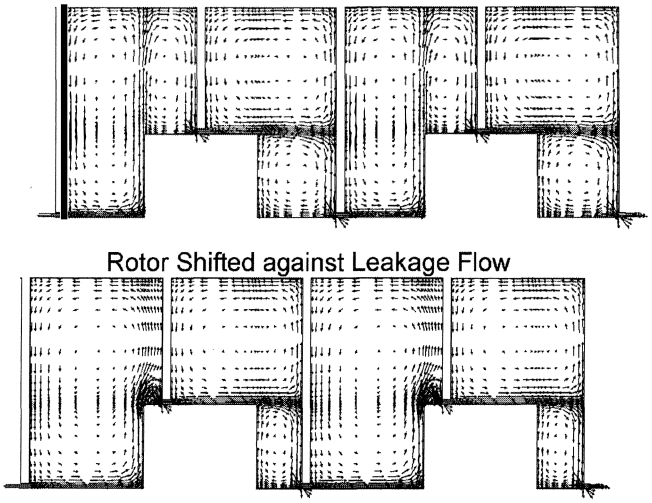

Figure 15. Flow Patterns within a Comb-Grooved Seal for Two Different Axial Rotor Positions.

Rotordynamic Calculations

An adaptation of the labyrinth seal coefficients was carried out in order to achieve a better coincidence with the measurements, especially with regard to the natural frequencies. The adaptation resulted in the following changes:

- Change of the sign of the direct stiffness in order to decrease the frequency with increasing pressure
- Doubling of the cross coupling damping in order to decrease the forward whirling frequency and to obtain a larger frequency split
- Doubling of the cross coupling stiffness in order to increase the forward whirling frequency in the case of no swirl brakes
- Doubling of the direct damping in order to increase the damping and to maintain the swirl frequency ratio constant

With these modifications, most of the measurements of ULA could be explained very well. Figure 16 shows a comparison of the measurement with the new calculation. To explain the physical background of the above described changes in the seal coefficients, it can be said that the order of magnitude of the coefficients depends very much on the actual clearance. Hence a doubling of the coefficients could be attributed to slightly smaller clearances during the tests compared with the calculation. The change of the sign of the direct stiffness has to be attributed to a still unknown effect within the comb-grooved labyrinth or within the shroud sideroom.

With these changes applied to the ALWYN rotor, it can be said that the measured frequency drop could be calculated quite well (much smaller frequency drops than ULA). But it did not have the desired effect on the damping. Further calculations showed that an increased cross coupling damping (negative values) not only decreases the forward whirling frequency, but also reduces the damping of the rotor. However, the calculations ended with the conclusion that, with these fixed modification factors, it will never be possible to predict all the observations.

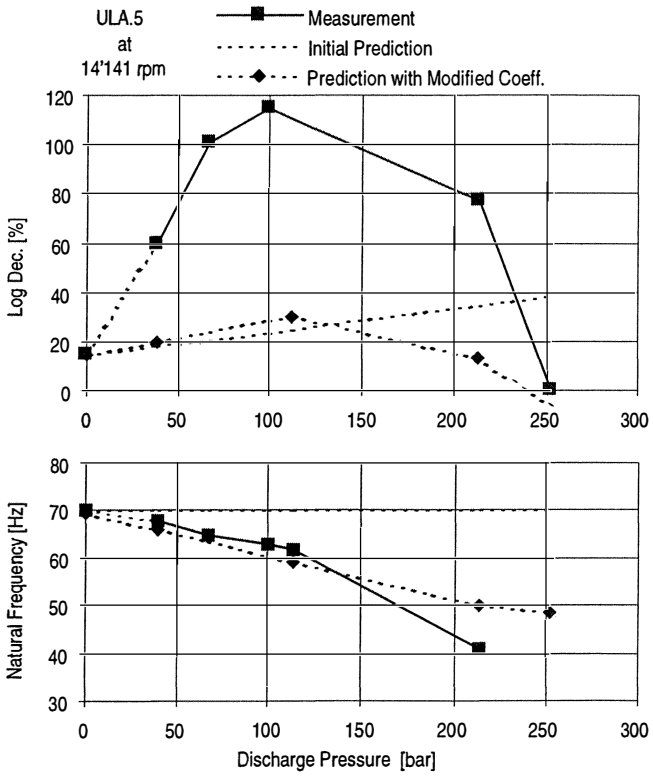

Figure 16. Comparison of the Measurement (ULA.5) to a Calculation with Modified Coefficients.

CONCLUSIONS

- In most of the investigated configurations, the measurements show a higher damping than the prediction. For the unstable configurations, the analytical determination of the threshold of stability was quite accurate.
- The measurements revealed a significant drop of the first natural frequency in all cases with many swirl brakes installed.
- This frequency drop is strongly correlated to the use of the comb-grooved labyrinths. Unfortunately this type of labyrinth has

a significantly lower leakage rate and represents the standard sealing for high-pressure compressors (at least at the balance piston).

- With a prediction that accounts for the observed effects, it would be possible to increase the efficiency of the compressor by approximately 5 percent to 10 percent.

- It is absolutely necessary to investigate alternative seal types. One of the possible alternatives is, for example, the honeycomb seal. An investigation program for this seal is presently running at Texas A&M University.

REFERENCES

Childs, D. W. and Scharrer, J. K., 1986a, "Experimental Rotordynamic Coefficient Results for Teeth-on-Rotor and Teeth-on-Stator Labyrinth Gas Seals," NASA CP 2443.

Childs, D. W., Scharrer, J. K., and Hale, K., 1986b, "Experimental Rotordynamic Coefficient Results for Sulzer Teeth-on-Stator Labyrinth Gas Seals," (321), TRC-Seal-3-86.

FVV Report, 1990, "Stroemungskraefte in Dichtlabyrinthen bei Radialer und Axialer Verschiebung des Rotors gegenueber dem Stator," Heft 452.

Nordmann, R. and Weiser, P., 1988, "Rotordynamic Coefficients for Labyrinth Seals Calculated by Means of a Finite Difference Technique," NASA CP 3026.

Weiser, H. P., 1989, "Ein Beitrag zur Berechnung der dynamischen Koeffizienten von Labyrinthdichtungssystemen bei turbulenter Durchstroemung mit kompressiblen Medien," Ph.D. Thesis, University of Kaiserslautern, Kaiserslautern, Germany.

Wyssmann, H. R., Pham, T. C., and Jenny, R. J, 1984, "Prediction of Stiffness and Damping Coefficients for Centrifugal Compressor Labyrinth Seals," ASME Journal of Engineering for Gas Turbines and Power, *106*, pp. 920-926.

ACKNOWLEDGEMENT

The author would like to take this opportunity to thank all those who made it possible to carry out these tests. Special thanks are expressed to BP Corporation and TOTAL Corporation who allowed us to modify and test their machines.